Royal Norwegian Council
for Scientific and Industrial Research
(NTNF)

NORSAR

NORSAR Scientific Report No. 1-90/91

Semiannual Technical Summary

1 April — 30 September 1990

Kjeller, November 1990

7.7 Optimal group filtering and noise attenuation for the NORESS and ARCESS arrays

A generalization of Capon's (1970) maximum likelihood technique for detection and estimation of seismic signals has recently been introduced by Kushnir *et al* (1990). By using a multidimensional autoregressive approximation of seismic array noise, a technique to use Capon's multichannel filter for online processing has been developed. Such autoregressive adaptation to the current noise matrix power spectrum has been shown to yield good suppression of coherent noise processes. This paper presents further results of our studies of of adaptive optimal group filtering (AOGF) which now has been applied to more than 80 earthquake and underground nuclear explosion recordings at the small aperture arrays NORESS and ARCESS in Norway (Fig. 7.7.1).

Compared to conventional beamforming, AOGF is demonstrated to provide high signal-to-noise ratio (SNR) gains (12–18 dB) over a wide frequency band (0.2–5.0 Hz), while retaining an undistorted signal waveform. This gain is mainly due to suppression of noise at low frequencies, where both noise power and noise coherency is greatest.

AOGF has also been tested in combination with statistically optimal algorithms for detection and onset time estimation using the maximum likelihood principle. Here, narrow-band filtering has been applied, selecting the frequency band most appropriate for detecting weak arrivals by conventional beamforming. Even in this case, AOGF provides significant gain in SNR (typically 6–8 dB in the 2–4 Hz band) compared to the array beam.

Description of software used

The conventional technique for array signal processing is based on beamforming, band pass filtering and STA/LTA detection. Beamforming is the statistically optimal procedure under the assumption of independent noise among the M different receivers of the array and in this case it improves power signal-to-noise ratio by a factor of M. For correlated noise this procedure is not optimal in the statistical sense. Bandpass filtering gives additional improvement of SNR, but this procedure, evidently, may reduce available information about the signals. The STA/LTA detector is a simple procedure, but it is sensitive only to variations of recorded power due to signal arrival, and it does not make use of spectral differences between signal and noise. So there is room left for improvement of this technique, and a possibility is to use statistically optimal procedures accounting for noise and signal features.

Now, at NORSAR a technique based on statistically optimal procedures has been tested. This technique is illustrated in Fig. 7.7.2 and consists of adapative optimal group filtering (AOGF) followed by optimal detection (OD) and optimal signal onset time estimation (OE) (see Pisarenko *et al*, 1987).

AOGF is based on a Wiener optimal filter with frequency response

$$\vec{H}(\lambda) = \vec{G}^*(\lambda)F^{-1}(\lambda)/\vec{G}^*(\lambda)F^{-1}(\lambda)\vec{G}(\lambda)$$

using the multichannel array record $\vec{X}_t = \vec{S}_t + \vec{\xi}_t$, $\vec{S}_t = \vec{\tilde{G}}_t^* u_t$ for input. The output of this filter Y_t is a scalar. AOGF reduces the noise power to a minimum, using the estimated inverse matrix power spectrum $F^{-1}(\lambda)$ of the array noise $\vec{\xi}_t$. The vector function $\vec{G}(\lambda)$ represents the medium frequency response along the paths from the seismic source to the array sensors, u_t is the scalar signal of the seismic source (waveform). For a homogeneous medium, $\vec{\tilde{G}}_t$ is determined by signal arrival delays at different stations. If AOGF is tuned properly ($\vec{G} = \vec{\tilde{G}}$) and $\vec{\xi} = 0$, then the AOGF output Y_t coincides with the signal waveform u_t. The procedure thus avoids introducing any distortion of the signal. If the noise is uncorrelated ($F(\lambda) = I$) (I - identity matrix) and $\vec{G}(\lambda)$ depends on delays only, then AOGF coincides with beamforming.

The inverse power spectrum matrix $F^{-1}(f)$ is estimated from pure noise preceding the signal by a procedure of adaptation using multichannel autoregressive (AR) modelling. AR estimation of this large size matrix function considerably reduces computations and has experimentally proved to be an excellent procedure for estimating the coherent noise matrix power spectrum.

The optimal detector (OD) (Fig. 7.7.2) is based on autoregressive modelling and moving window detection. In a series of experiments OD proved to exceed STA/LTA results due to optimal accounting of spectral variations in the moving window. The optimal estimator (OE) (Fig. 7.7.2) is a maximum likelihood procedure applied to the time interval around the detection time. It is likewise based on an autoregressive modelling procedure and is sensitive to small variations of spectra in a chosen time interval.

Coherency of noise and optimal group filtering

In Kushnir and Lapshin (1984) it is shown that the SNR at the output of OGF tends to infinity with increasing noise coherency. Coherent noise may be represented as a superposition of noise contributions from several spatially distributed sources. ARCESS and NORESS noise seems to have a strong coherent component, which made it possible to achieve power SNR gain factors of AOGF relative to beamforming of about 70–80 at ARCESS and 20–30 at NORESS (Kushnir *et al*, 1990; Kushnir *et al*; 1989). Coherent noise may be recognized from spatial spectral FK-analysis, where noise and signals coming from different sources correspond to different peaks in the slowness vector plane. Strong coherent noise may be represented in the frequency domain as

$$\vec{\xi}(\lambda) = \sum_{k=1}^{N} \xi_k(\lambda)\vec{\phi}_k + \epsilon\vec{\eta}(\lambda), \qquad \lambda \in (0, 2\pi]$$

where $\xi_k(\lambda)$ are scalar noise source signals, $\vec{\phi}(\lambda)$ is the vector frequency response from the k-th noise source to the array receivers, and $\vec{\eta}(\lambda), k = 1, \ldots, N$

are independent power spectrum matrices.

$$F(\lambda) = \sum_{k=1}^{N} f_k(\lambda)\vec{\phi}_k(\lambda)\vec{\phi}_k^*(\lambda) + \epsilon^2\Phi(\lambda) \qquad (1)$$

where $f_k(\lambda)$ is the spectral density of $\xi_k(\lambda)$ and $\Phi(\lambda)$ is the matrix power spectrum of diffuse noise, and $\vec{\phi}_k^*$ is the transposed conjugated vector. It can be seen that if $\epsilon \to 0$, the matrix $F(\lambda)$ projects each vector signal $\vec{Q}(\lambda)$ recorded by the array to the "noise" subspace, i.e., linear subspace

$$\left\{\vec{\phi}_k(\lambda),\ k = 1, \ldots, N\right\}:$$

$$f(\lambda)\vec{Q}(\lambda) \underset{\epsilon \to 0}{\longrightarrow} \sum_{k=1}^{N} C_k\vec{\phi}_k(\lambda)$$

and $F^{-1}(\lambda)$ projects $\vec{Q}(\lambda)$ to the orthogonal subspace $\{\phi_k(\lambda)\}^{\perp}_{k=1,\ldots,N}$. Hence, the power of each signal, coming from the "noise" subspace, will be greatly reduced by OGF. We would like to note that compensation of noise by OGF does not require stationarity of the noise source signals $\xi_k(\lambda)$, but stationarity of $\vec{\phi}(\lambda)$ is important.

Description of experiments

Checking of noise attenuation stability. This paper is the second report concerning our attempts to use AOGF at NORSAR. In the first one (Kushnir *et al*, 1989), we described theoretical capabilities of AOGF and its successful application for broad band extraction of one of the smallest nuclear explosion signals recorded at ARCESS. But in the case described in Kushnir *et al* (1989), adaptation was done just before the onset time. Therefore some doubts remained as to whether AOGF would work continuously without losing its good features during long periods of filtering time. To check the AOGF performance stability, we applied AOGF to some long-term records of pure ARCESS and NORESS noise.

In Fig. 7.7.3 we show the results of filtering by AOGF the 25 channels of a 40- minute long NORESS noise record. Only the first 2 minutes of the time interval were used for adaptation. AOGF output noise power is gradually increasing, but SNR power gain relative to the beam does not become less than 20. It means that if a signal arrives during this time interval, its SNR will be enhanced by AOGF at least 20 times better than by the beam. Looking at Fig. 7.7.3, one may predict that OGF can work much better than the beam during one hour or even more.

We applied AOGF to 5 ARCESS and 5 NORESS records each consisting of 25 minutes of pure noise, computing the SNR power for each 5 minutes. The results are presented in Fig. 7.7.4. From Fig. 7.7.4b we see that the gain of AOGF relative to beamforming for NORESS is between 15 and 25, for

ARCESS from 30 to 75. Again, adaptation is done during the first 2 minutes, and that is why we have the largest gain for the first 5 minutes, including the interval of adaptation. AOGF includes two stages: adaptation and filtering. The first is time consuming, the second is not. If readaptation is only needed once an hour or so, one may attempt to use several AOGFs, tuned to different azimuths and apparent velocities in the same manner as done by beamforming at NORSAR, and this may be more effective for noise suppression in online processing. An illustration of such an application of AOGF is shown in Fig. 7.7.5, where the gain of AOGF is presented versus azimuth. The velocity is constant and equal to 13 km/sec. The peak of the gain corresponds to the southern direction.

Extraction of missed phases. The capability of AOGF to work for a long time without readaptation also makes it possible, using pure noise before P arrivals for adaptation, to enhance the SNR of seismic phases located in time far from the P arrival. Two examples, described below, illustrate the application of all three optimal algorithms: adaptive optimal group filtering, optimal detection, and onset time estimation for extraction of missed seismic phases. It sometimes happens that regional phases like Pn or Lg are missed by the detector applied at NORSAR in the regular processing of NORESS and ARCESS data. We tried to use AOGF, OD and OE to remedy this situation for some of these cases, and they seemed to work well. Two cases were considered.

a) For case 1 (Fig. 7.7.6a), the Lg phase was detected on NORESS, but the Pn and Sn phases were missed. Fig. 7.7.6b shows data for the same event, as recorded on the FINESA array in Finland. In Fig. 7.7.6c the result of AOGF, OD and OE and beamforming are shown for a window containing the presumed Pn onset. The onset time of the Pn wave is clearly seen, and the maximum of the OE curve is close to the theoretical Pn arrival. (The theoretical Pn arrival time is computed from the event location derived from the FINESA array data.) The theoretical and experimental P arrivals are shown on Fig. 7.7.6a. The first detection shown in Fig. 7.7.6d is questionable (is it caused by the Sn phase from the event considered or not) because the theoretical Sn arrival time differs from the experimental one. The second detection in Fig. 7.7.6d is more likely related to the Sn phase from the event considered.

b) For case 2 (Fig. 7.7.7a) the regular NORESS processing detected the Pn and Sn phases, but no Lg was detected. This interpretation is confirmed by inspecting the ARCESS records. We have done an adaptation for AOGF just before the Pn arrival. The results are shown in Fig. 7.7.7b, where all three phases Pn, Sn and Lg are evidently detected. Their arrival times are shown on Fig. 7.7.7a as well.

These results suggest possible applications of AOGF in combination with

OD and OE for improvement of the detection lists generated by NORSAR's regular processing of array data.

Adaptive group filtering of seismic signals

AOGF was applied to the processing of 35 teleseismic earthquakes and 44 nuclear explosion signals recorded at NORESS. Earthquake locations are shown in Fig. 7.7.8. Most of the explosions are located at the Shagan River site. This selection of events was made with a view to future work on the discrimination problem. In all the cases, the SNR was much improved by AOGF, but the events may be divided into two classes. One class is where SNR was small in the first place and the other where it was large. In the first class (example in Fig. 7.7.9) improvement of SNR by AOGF is evident, and in the other example (Fig. 7.7.10a) the improvement is not evident in a broad frequency band (0.2–5.0 Hz). But if we consider only the low frequency band (for example, 0.2–0.5 Hz) the advantage of the group filter is seen clearly (Fig. 7.7.10b). This is due to two factors: The first is that at this latter frequency band the SNR is worse for the short-period records used, and the second is that the gain of AOGF seems to be largest due to the high noise coherency in this band.

Conclusion

By application of advanced techniques (apative optimal group filtering, optimal detector, optimal estimator), based on statistical algorithms, processing of NORESS and ARCESS array data may be improved. This improvement could be achieved by taking optimal advantage of array noise coherency and signal frequency contents. Compared to conventional beamforming, AOGF is demonstrated at NORESS and ARCESS to provide SNR gains from 12 to 18 dB over a wide frequency band from 0.2 to 5 Hz, while retaining an undistorted signal waveform. This gain is mainly due to suppression of noise at low frequencies, where both noise power and noise coherency is greatest. But even for the frequency band from 2 to 4 Hz, AOGF provides a typical gain in SNR of the order 6 to 8 dB compared to the array beam. The performance of AOGF appeared to be stable in time without need for readaptation, for time intervals at least one hour long. This may result in possible application of AOGF to supplement conventional beamforming for online signal detection and extraction. The proposed technique may be utilized also in post-processing for detecting and onset time estimating of seismic phases missed by conventional methods. As a result, it may reduce the detection threshold and improve the reliability of event detection and location using array signals.

A.F. Kushnir, V.I. Pinsky, S. Tsvang, Int. Inst. of Earthquake Prediction Theory, Moscow, USSR
J. Fyen, S. Mykkeltveit, F. Ringdal, NORSAR

References

Capon, J. (1970): Application of signal detection and estimation theory to the large array seismology. *Proc. IEEE*, Vol. 58, 170–186.

Kushnir, A.F. and V.M. Lapshin (1984): Optimal processing of the signals received by a group of spatially distributed sensors. *Computational Seismology*, Vol. 17, Allerton Press, Inc., 163–174.

Kushnir, A.F., V.I. Pinsky and J. Fyen (1989): Statistically optimal event detection using small array data. *Semiannual Technical Summary, 1 April - 30 September 1989*, NORSAR Sci. Rep. 1-89/90, Kjeller, December 1989.

Kushnir, A.F., V.M. Lapshin, V.I. Pinsky and J. Fyen (1990): Statistically optimal event detection using small array data. *Bull. Seism. Soc. Am.*, 80, in print.

Pisarenko, V.F., A.F. Kushnir and I.V. Savin (1987): Statistical adapative algorithms for estimation of onset moments of seismic phases. *Phys. Earth Planet. Inter.*, 47, 4–10.

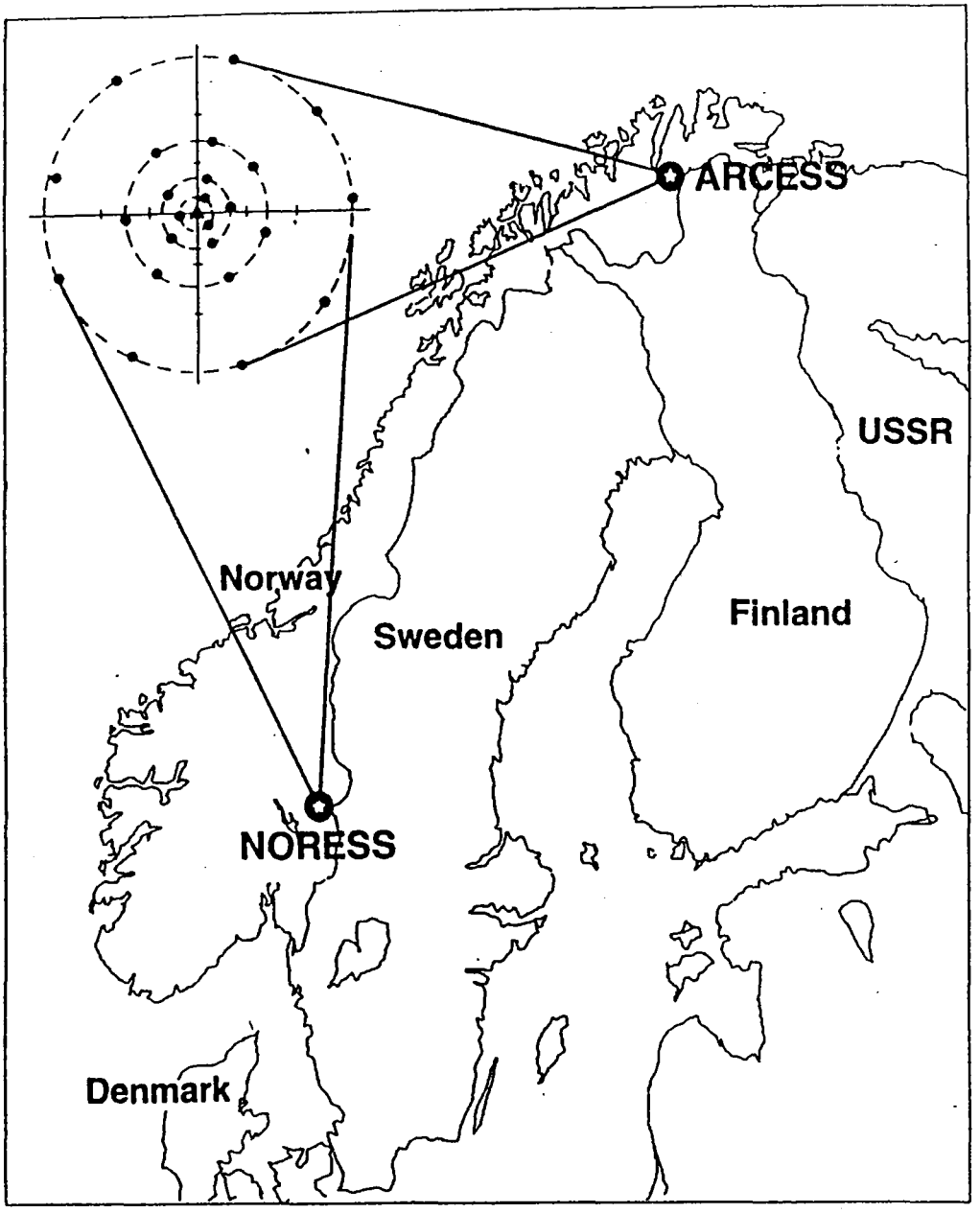

Fig. 7.7.1. The locations and array geometry for the NORESS and ARCESS arrays. The two arrays are essentially identical, each having 24 elements in four concentric rings (A, B, C, D) plus a center element (A0). The diameter of the outer (D) ring is 3.0 km. There are 3-component seismometers at A0 and three of the seven sites in the C-ring.

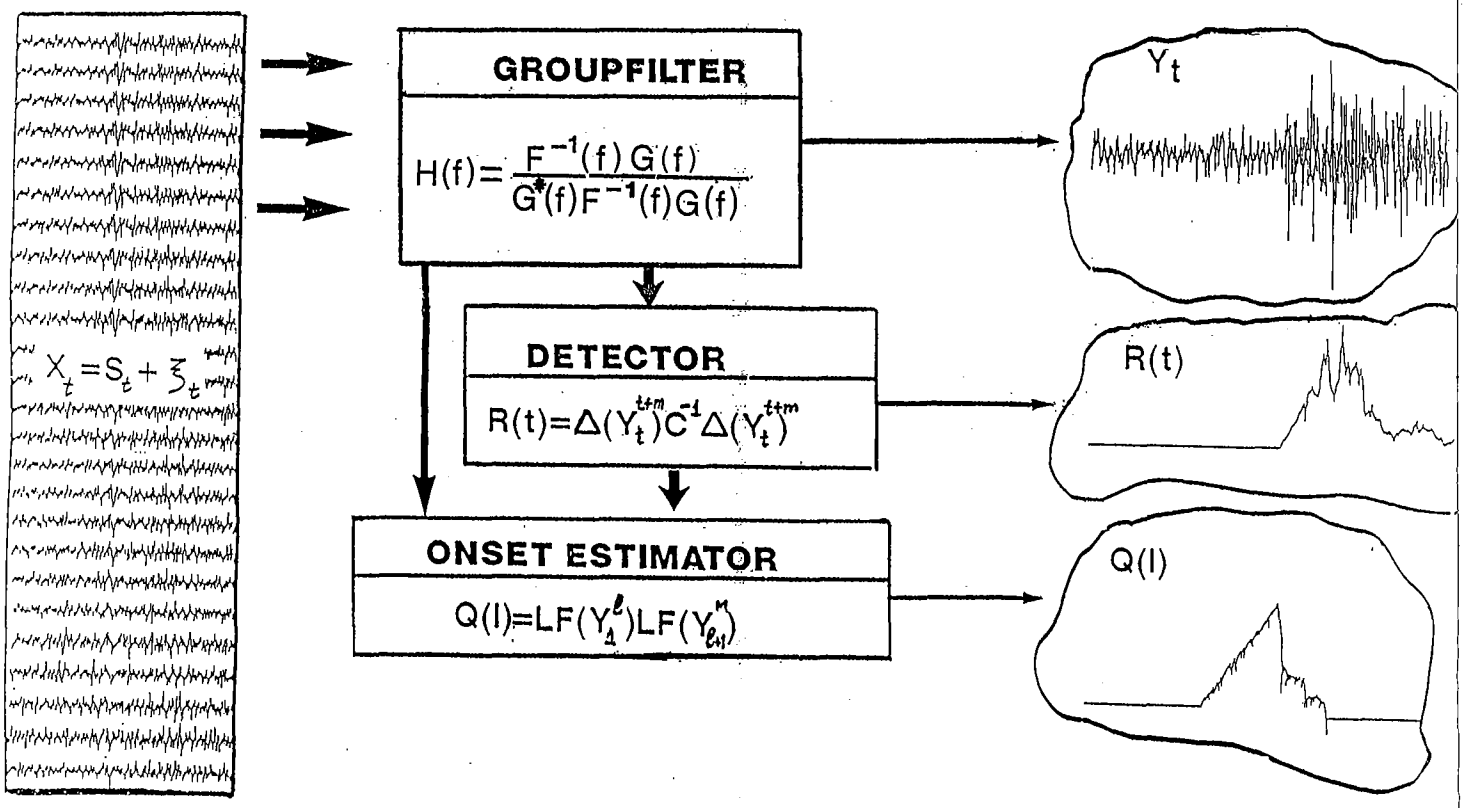

Fig. 7.7.2. Statistically optimal algorithms for preliminary array signal processing. X_t — multichannel seismic record; S_t — signal; ξ_t — noise; $H = H(\lambda)$ — frequency response of OGF; $F^{-1} = F^{-1}(\lambda)$ — inverse matrix power spectrum; $G = G(\lambda)$ — vector medium frequency response; Y_t — scalar output of AOGF, $R(t)$ — detector statistic; Y_t^{t+m} — observations in moving window (width = m samples); Δ — asymptotically sufficient statistics; C^{-1} — inverse covariance matrix of Δ computed at adaptation step; $Q(\ell)$ — likelihood function of onset time t_e; LF — likelihood functions of observations $Y_1^\ell = (Y_1, \ldots, Y_\ell), Y_{\ell+1}^M = (Y_{\ell+1}, \ldots, Y_M)$.

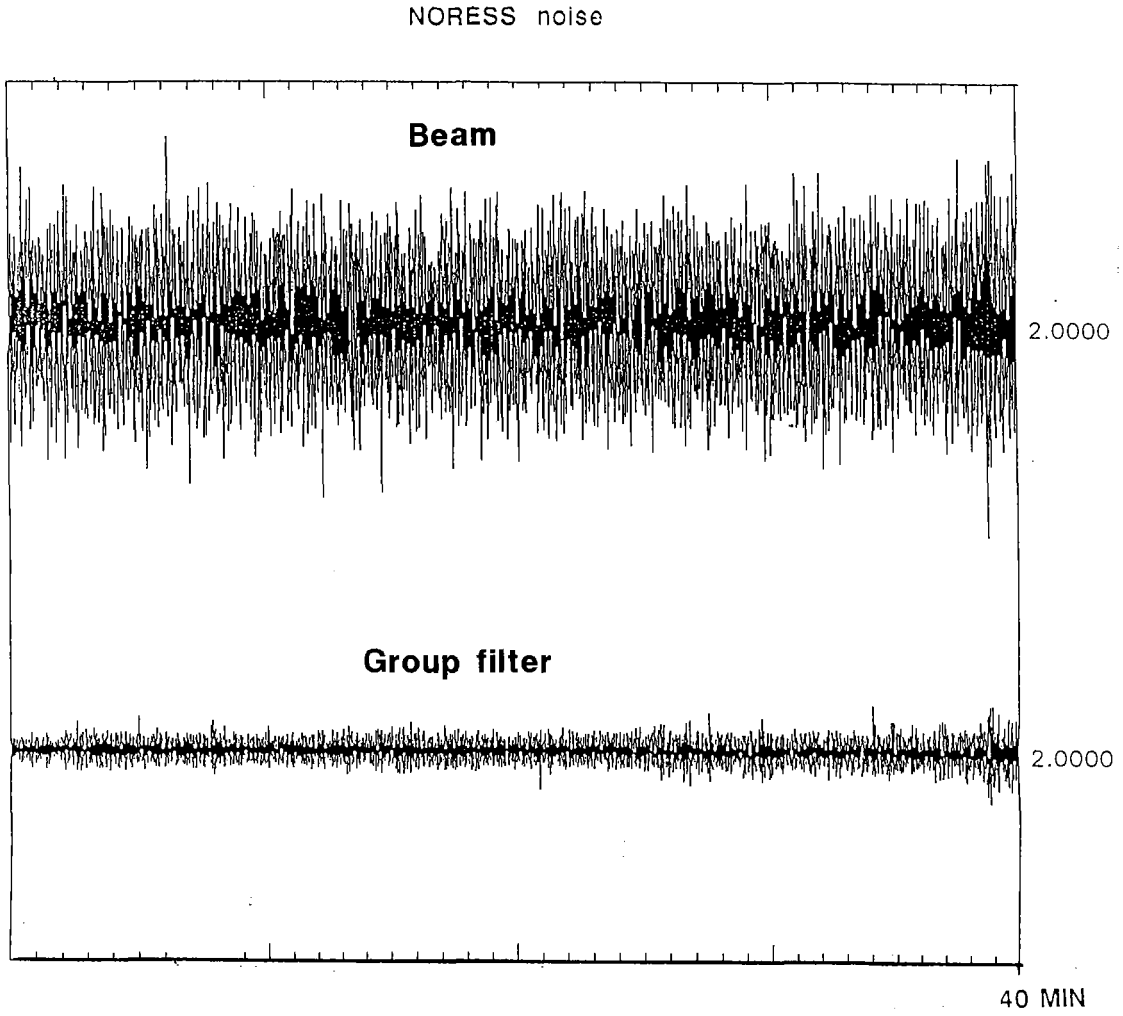

Fig. 7.7.3. 40 minutes of pure NORESS noise filtered by beam and optimal group filter in the same scale.

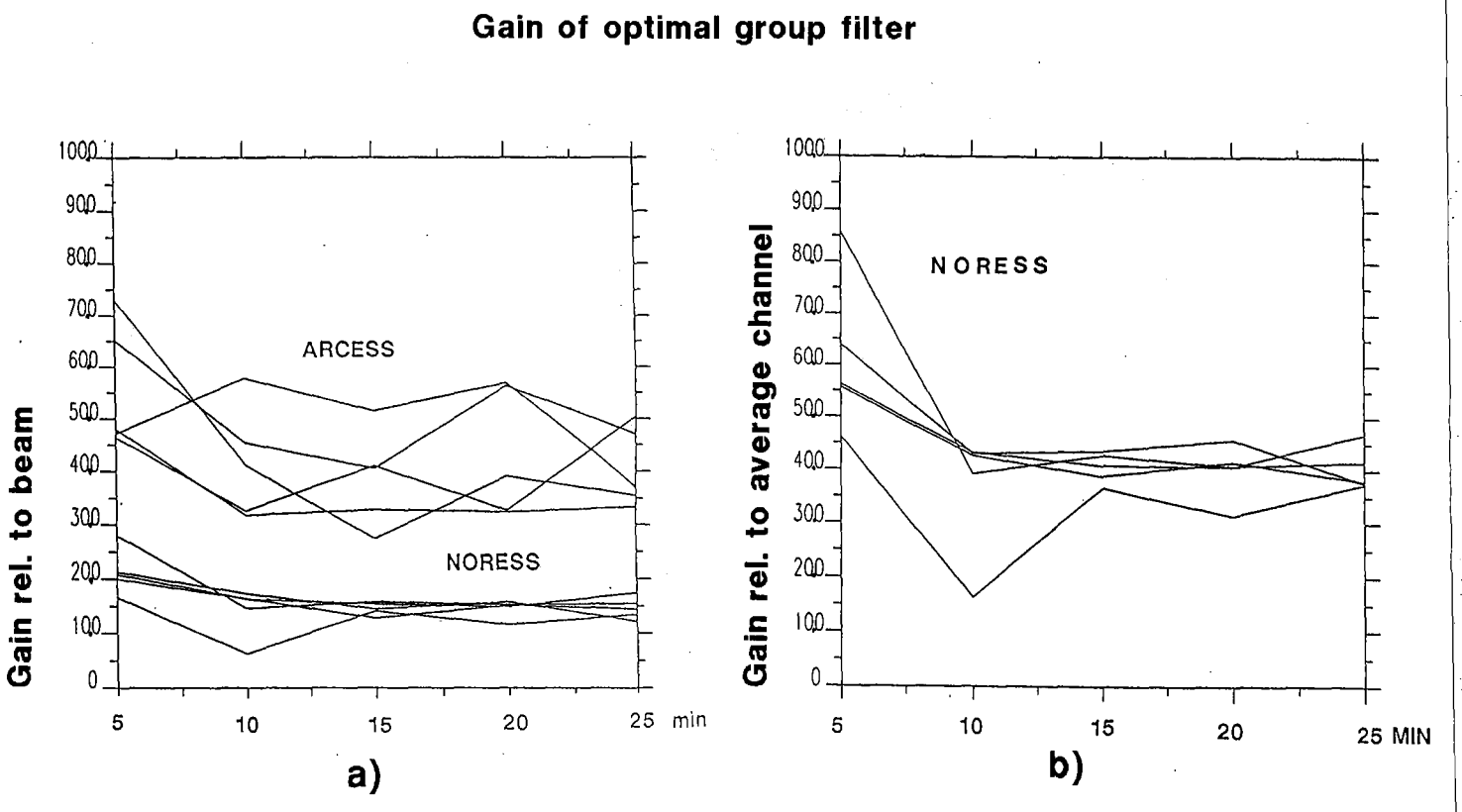

Fig. 7.7.4. Power SNR gain of optimal group filter computed each five minutes: a) relative to beamforming; and b) relative to average NORESS channel.

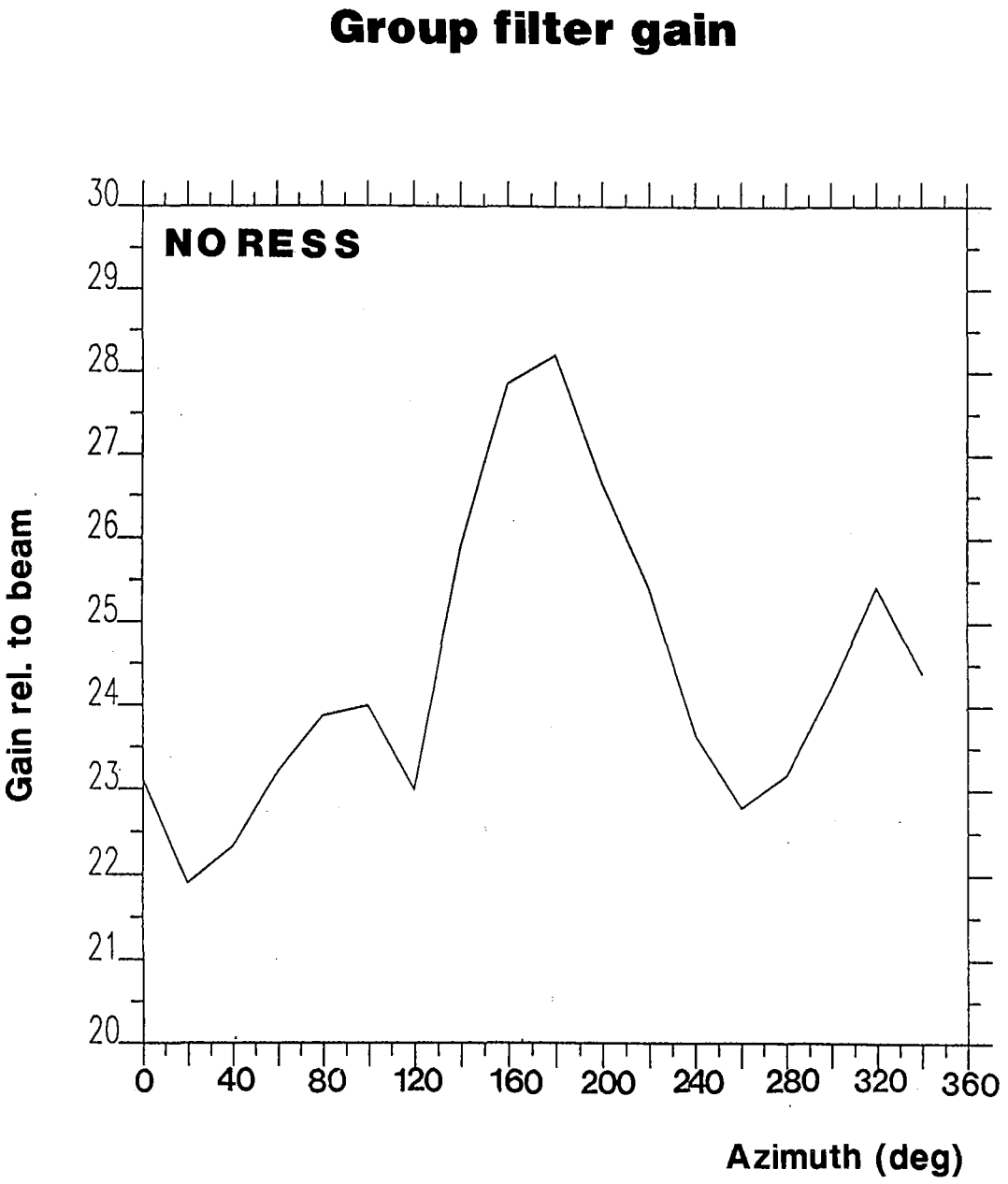

Fig. 7.7.5. Group filter gain for pure noise versus azimuth. The apparent velocity is equal to 13 km/sec. The maximum corresponds to the southern direction.

NORESS data. No Pn detection on NORESS. Only Lg detected.

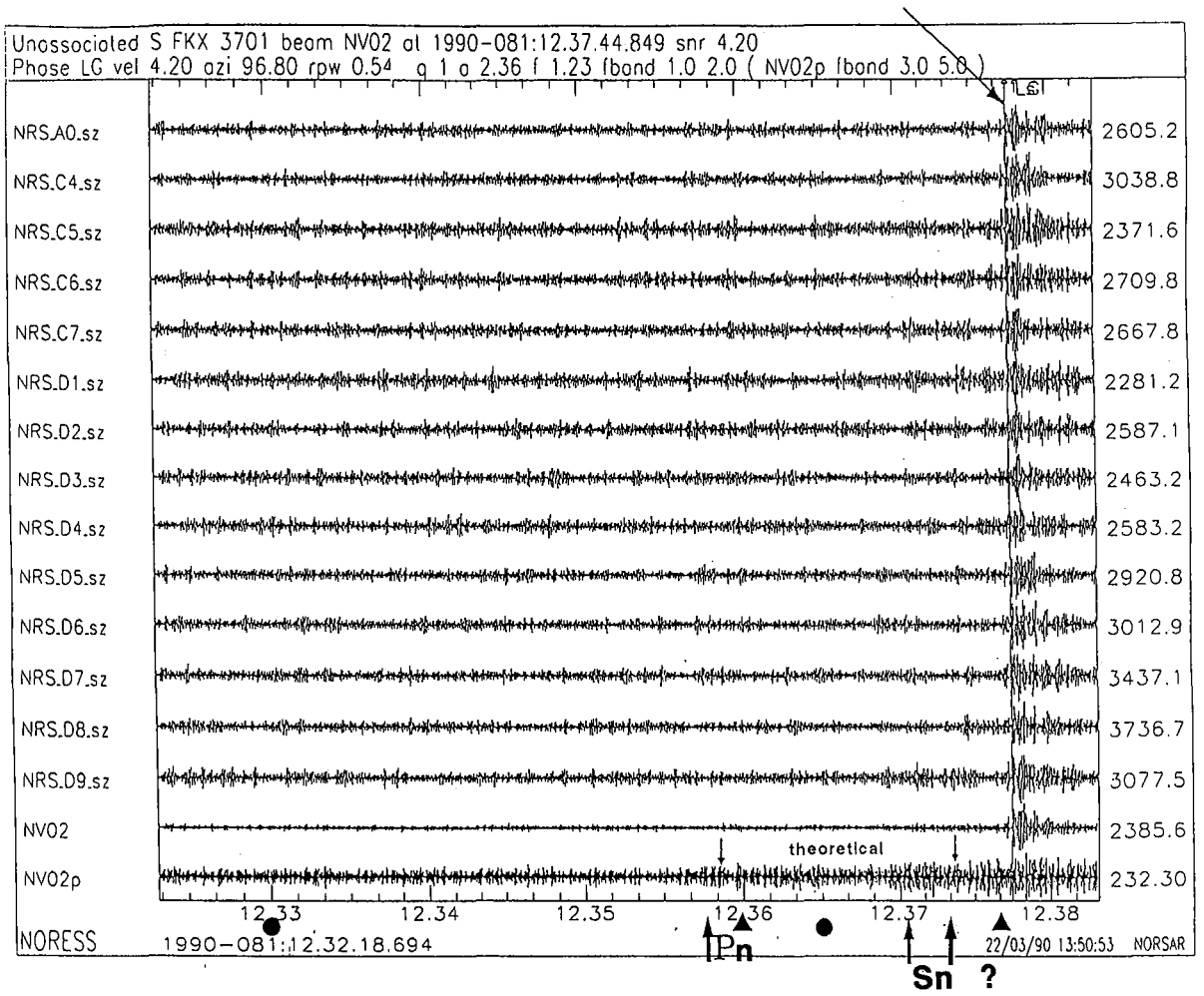

Fig. 7.7.6a. Illustration of the AOGF, OD and OE procedures as applied to NORESS data for a small event in Estonia, from which only the Lg phase was detected by the regular processing at NORSAR of NORESS data. The arrows show theoretical and computed (by the OE procedure) arrival times for Pn and Sn phases. Circles mark the time interval, in which there was a search for a Pn phase (see Fig. 7.7.6c), triangles mark the interval for searching for the Sn phase (see Fig. 7.7.6d).

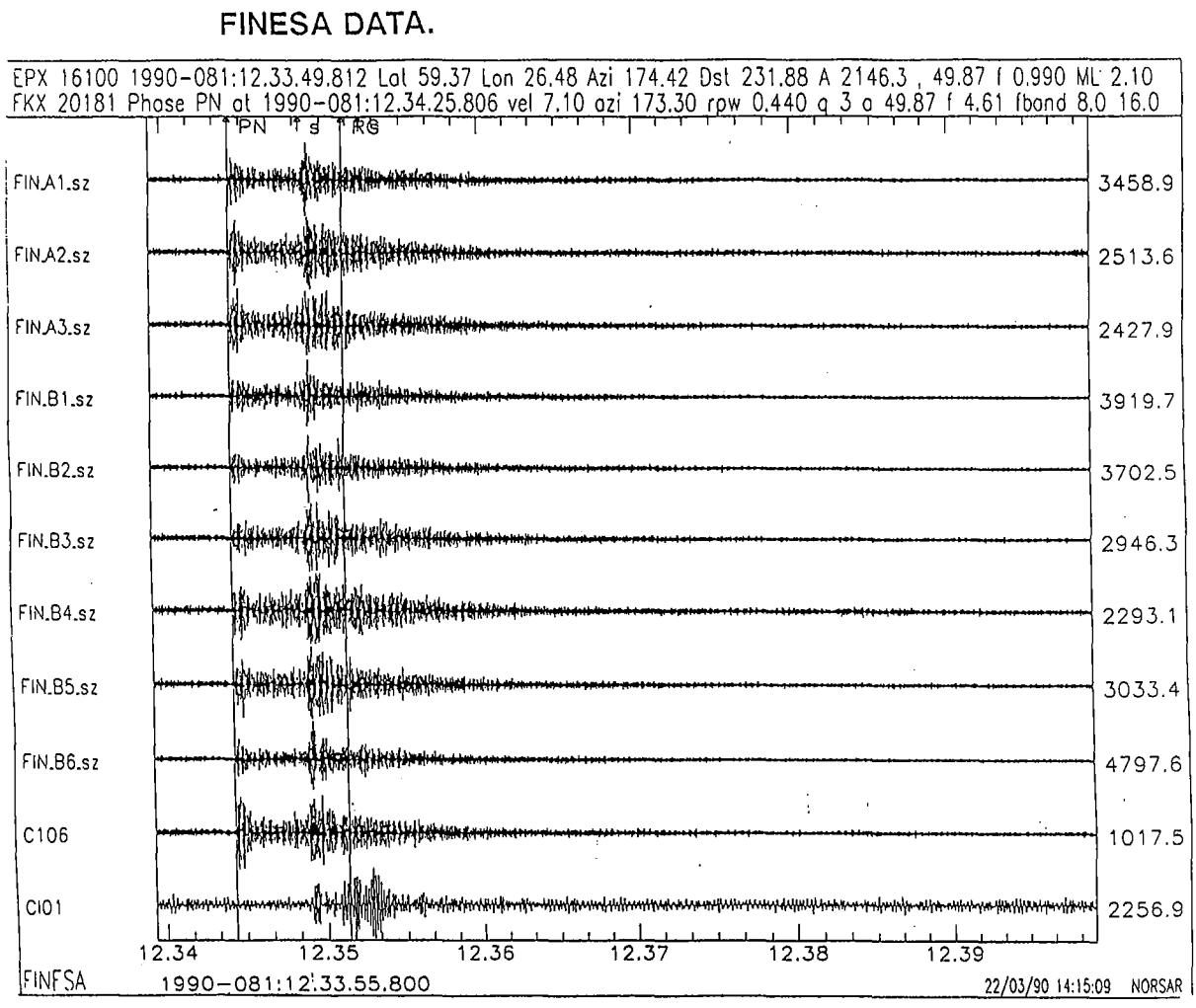

Fig. 7.7.6b. FINESA recording of the event for which Lg at NORESS is seen in Fig. 7.7.6a.

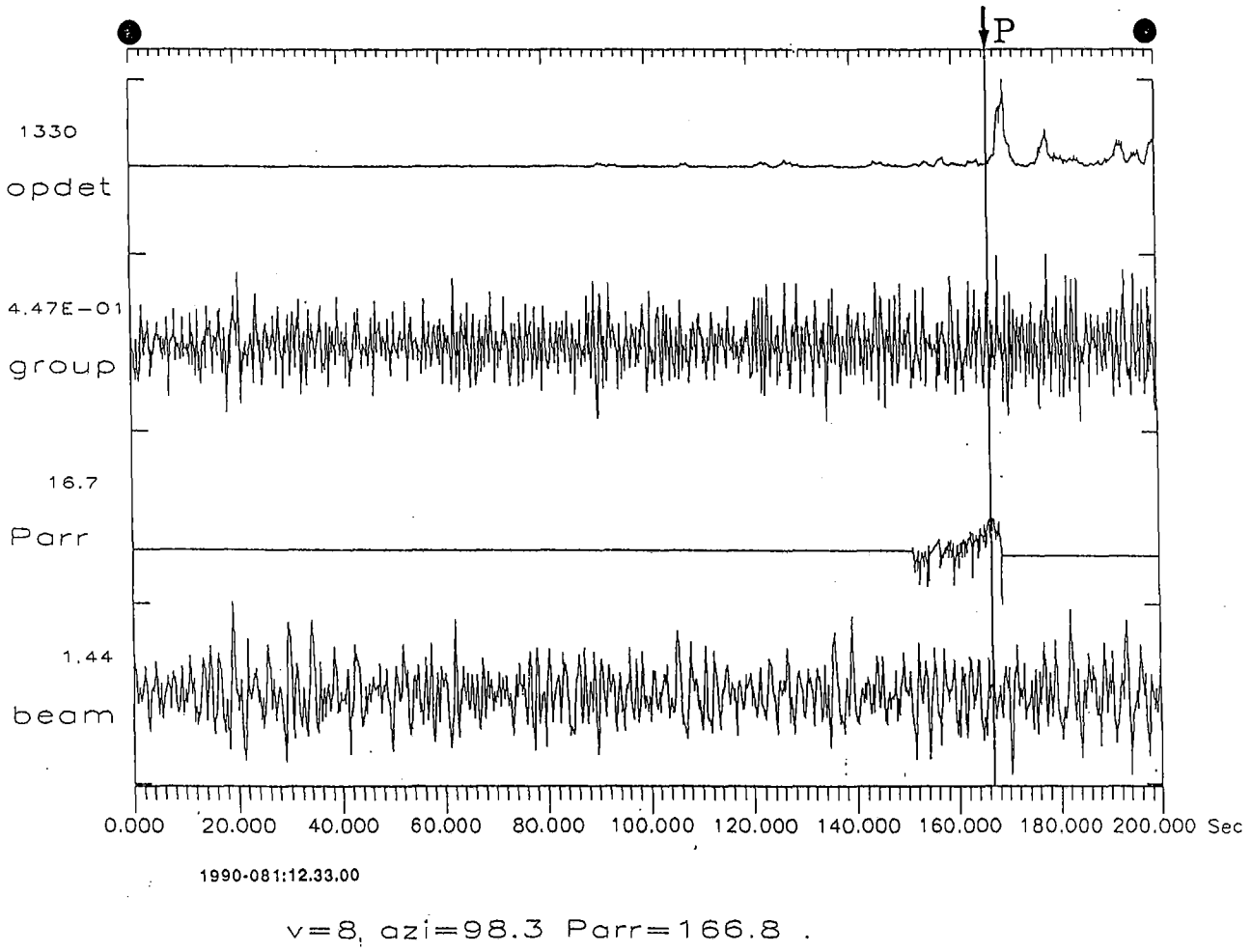

Fig. 7.7.6c. NORESS Pn-wave detection and onset estimation performed on AOGF output data. "V" and "AZI" correspond to apparent velocity and azimuth used in AOGF, "Parr" is computed by OE relative to the beginning of the interval for the search for the Pn phase.

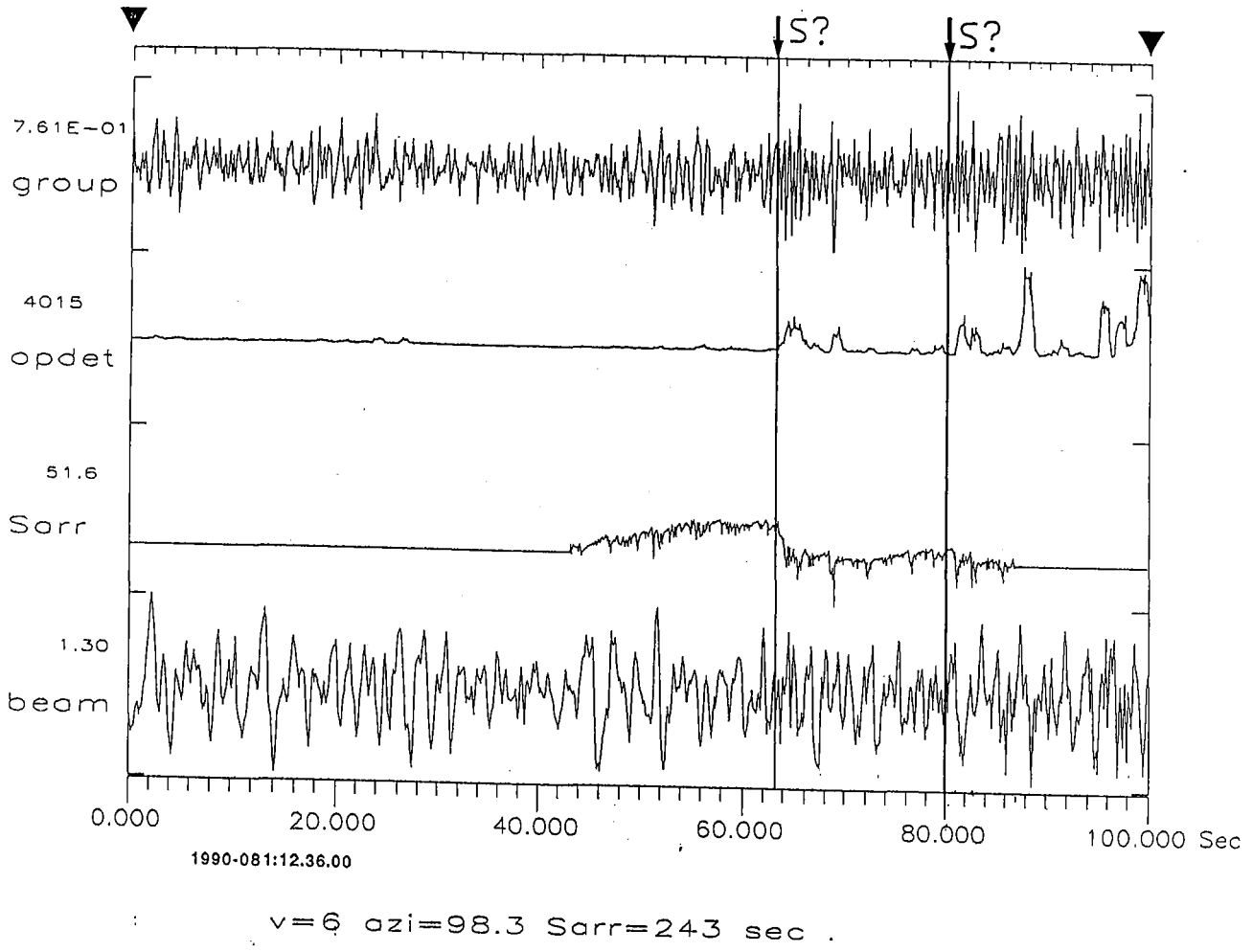

Fig. 7.7.6d. NORESS Sn-wave detection and onset estimation performed on AOGF output data. "V" and "AZI" correspond to apparent velocity and azimuth used in AOGF, "Sarr" is computed by OE relative to the beginning of the interval for the search for the Pn-phase.

NORESS data. No Lg detected on NORESS.

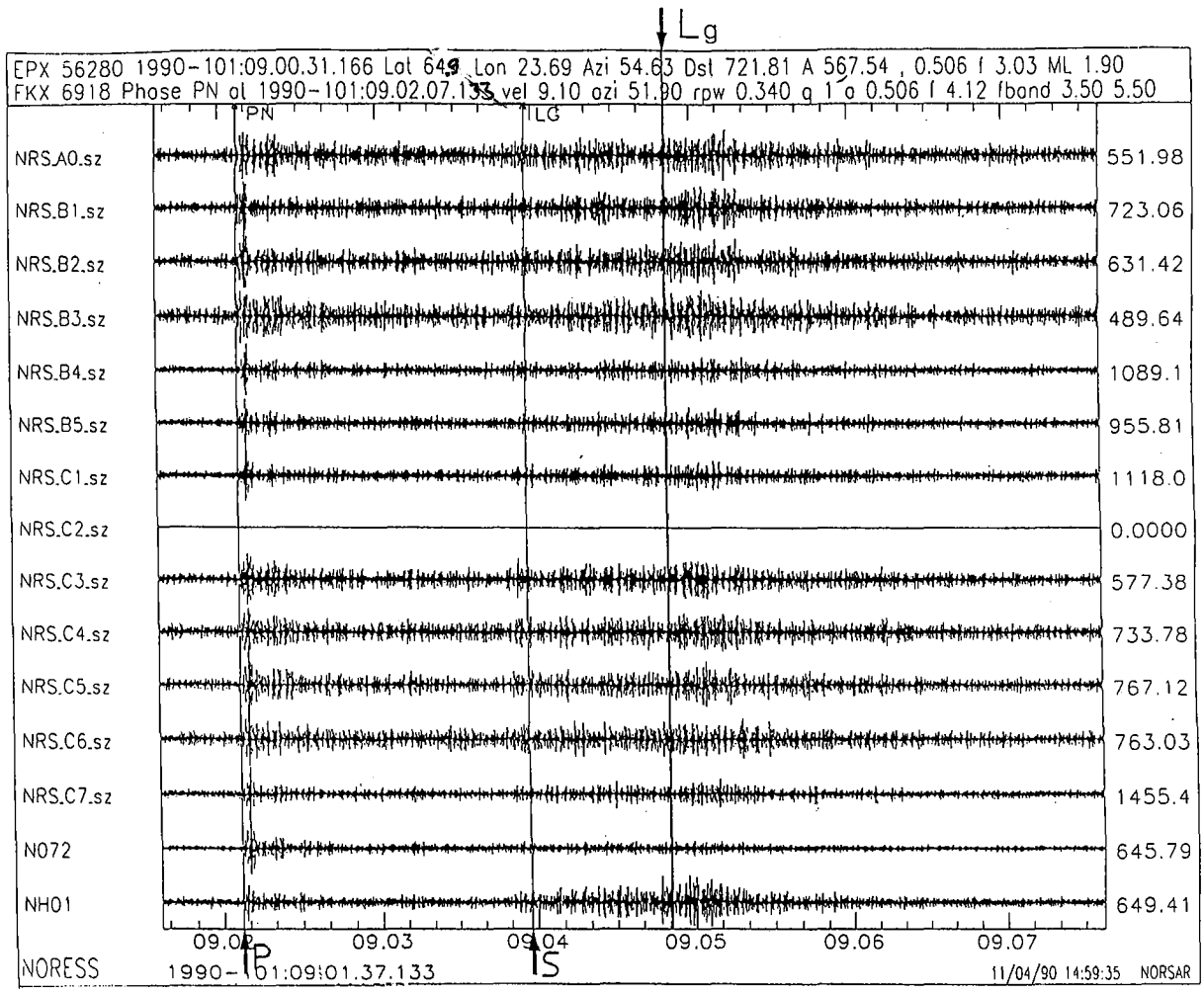

Fig. 7.7.7a. Illustration of the AOGF, OD and OE procedures as applied to an event from the USSR/Finland border region, for which the Lg phase was not detected by the NORESS regular processing. (The Sn phase at approximately 09.04 was detected, but incorrectly assigned as Lg.) Arrows show estimates of arrival times, using the OE procedure.

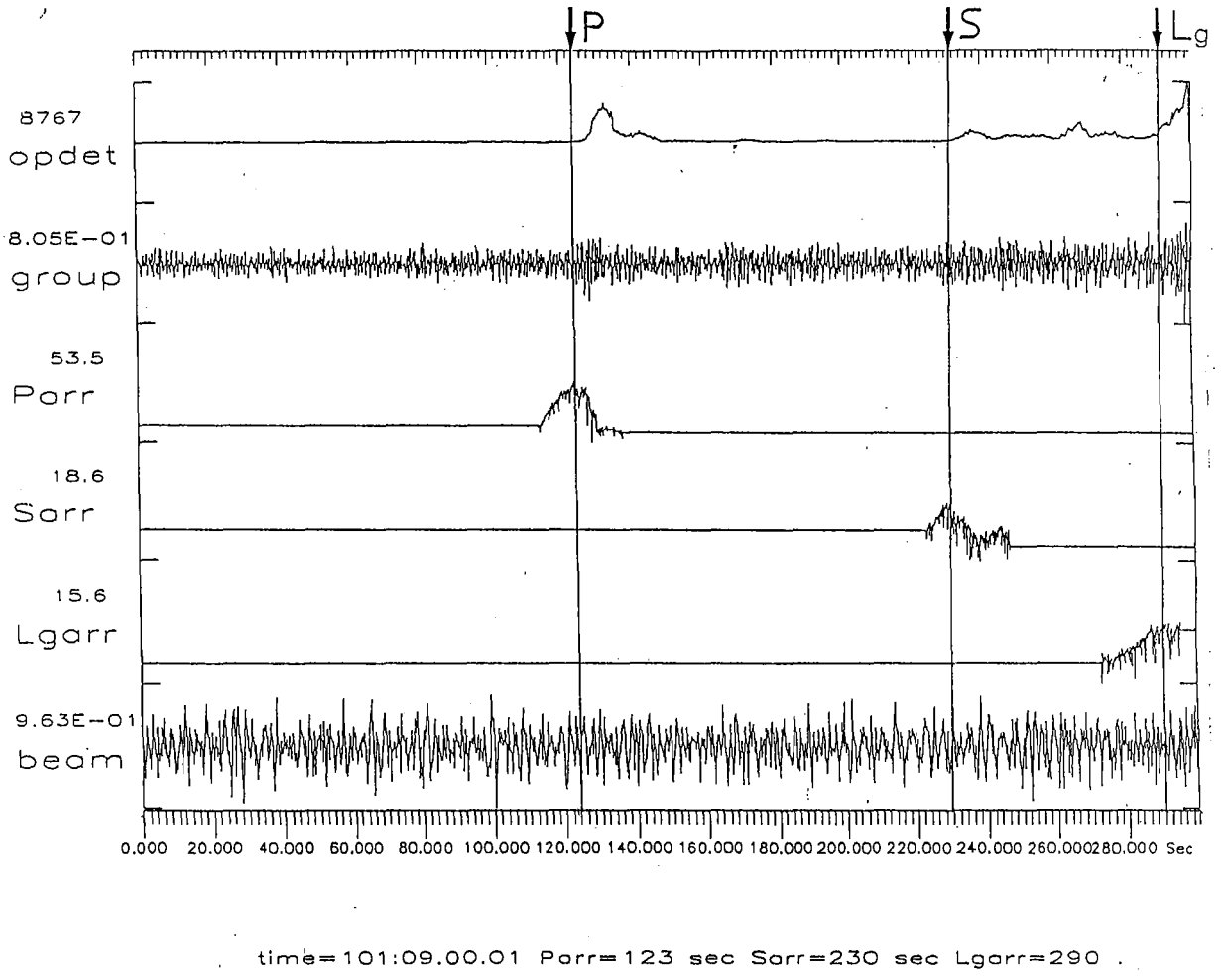

Fig. 7.7.7b. Pn, Sn and Lg detection and estimation performed on AOGF output data. "Time" gives the time of the beginning of the adaptation. "Parr", "Sarr" and "Lgarr" are computed by OE relative to the beginning of the interval.

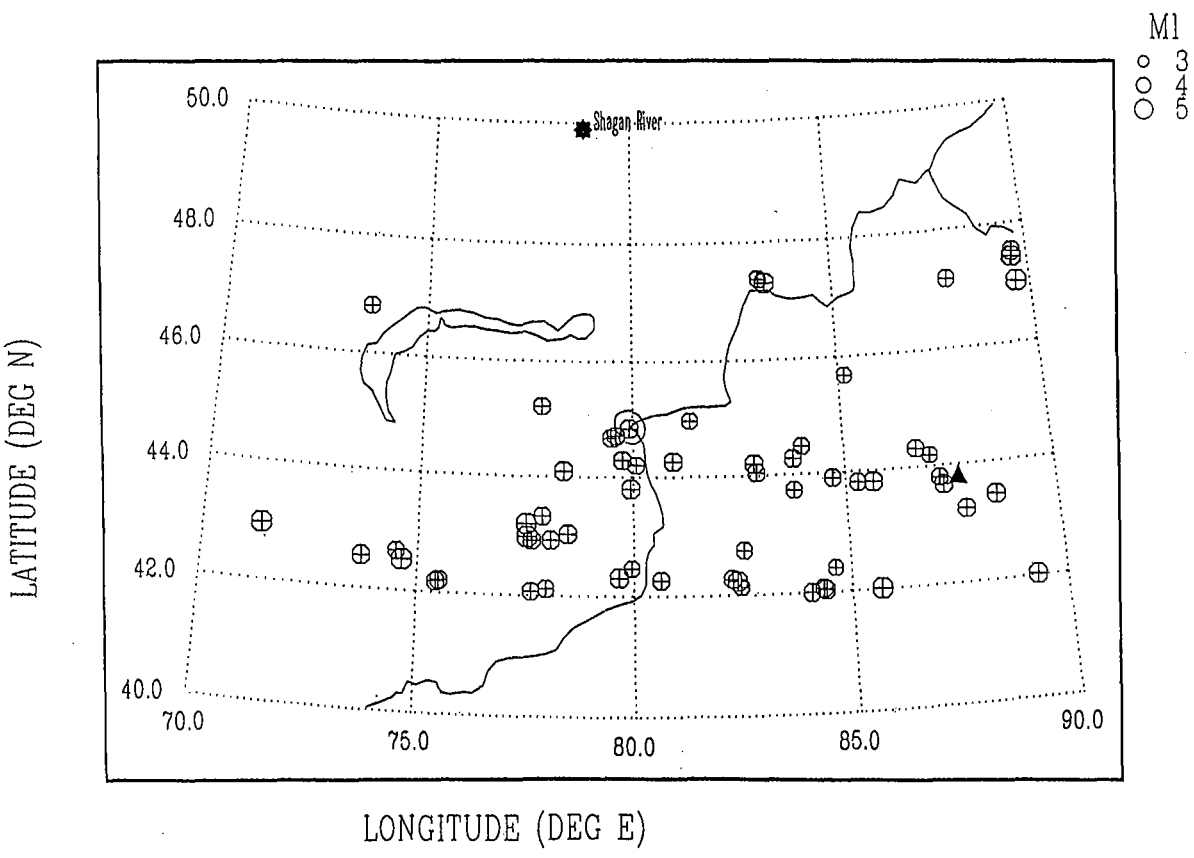

Fig. 7.7.8. Map showing the location of 35 earthquakes used in this study. Most explosions used are located at the Shagan River site.

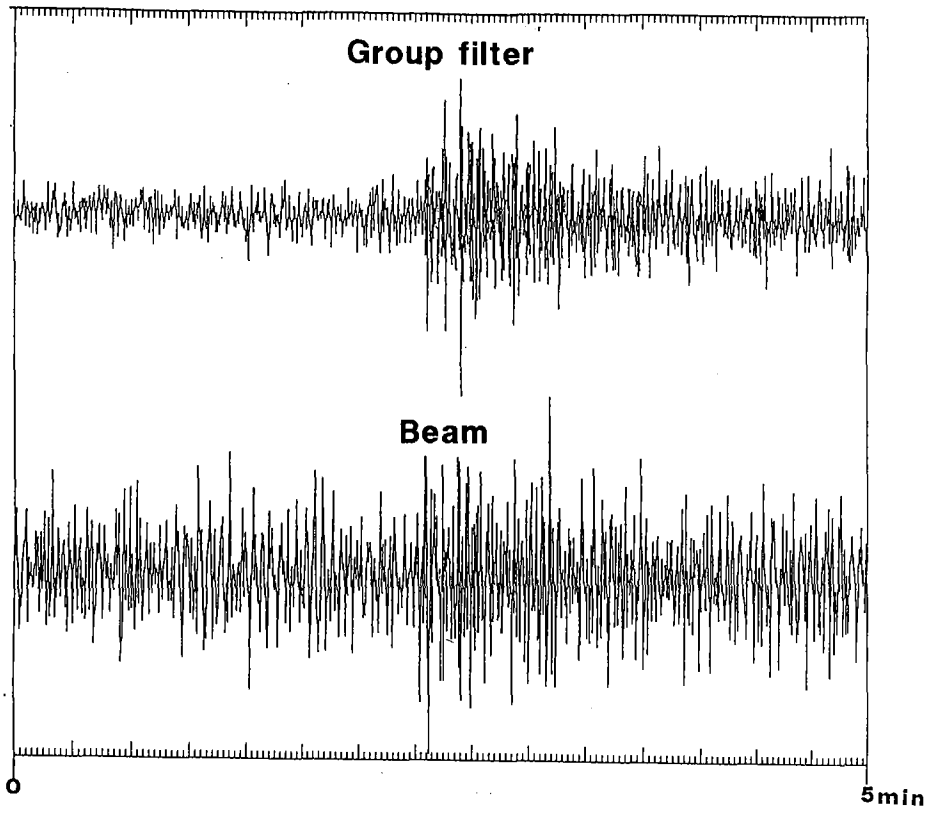

Fig. 7.7.9. Example of earthquake record filtered by beam and AOGF.

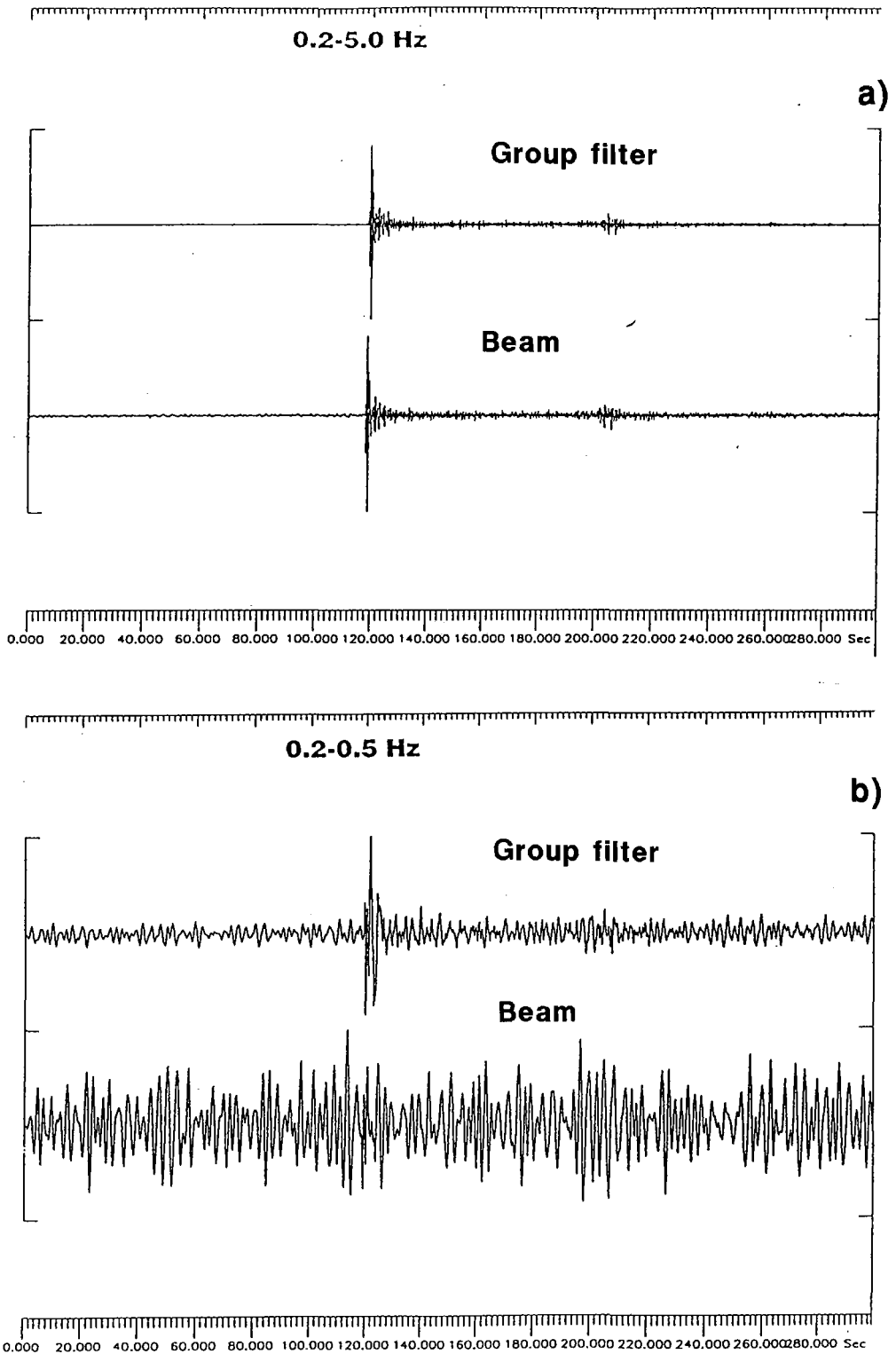

Fig. 7.7.10. Example of nuclear explosion record filtered by beam and AOGF in: a) broad frequency band and b) low frequency band.